# 15

# The Effects of Trimethylamine N-Oxide on the Structural Stability of Prion Protein

Barbara Yang, Kuen-Hua You,
Shing-Chuen Wang, Hau-Ren Chen and Cheng-I Lee
*Department of Life Science, National Chung Cheng University*
*Taiwan,*
*ROC*

## 1. Introduction

Transmissible spongiform encephalopathies (TSEs) are diseases that affect the central nervous system in both humans and animals. TSEs can be ascribed to conformational conversion of prion protein (PrP). "Prion" stands for "proteinaceous infectious particle", which was discovered in the disease-transmitting material of infectious brain tissues and named by Prusiner (Prusiner 1982). The normal, cellular form of PrP ($PrP^C$) is a α-helix-rich glycoprotein attached to the outer cell surface by a glycophosphatidyl inositol linkage. The biological role of $PrP^C$ remains ambiguous. Since $Cu^{2+}$ is unique among divalent metal ions in its ability to bind to $PrP^C$ in the octarepeat region (four copies of the repeat ProHisGlyGlyGlyTrpGlyGln) in the N-terminal domain (Whittal et al. 2000), the prion protein has been suggested to play a role in maintaining cellular copper concentration and signal transduction (Brown et al. 1998; Mouillet-Richard et al. 2000). $PrP^C$ is non-infectious, whereas the abnormal and infectious, Scrapie isoform of PrP ($PrP^{Sc}$) has been considered to be the major infectious component of the genetic, sporadic and transmissible fatal neuro degenerative prion diseases that affect both human and animals (Prusiner 1998). $PrP^{Sc}$ is rich in β-sheet structures and it has a pronounced tendency to misfold and to subsequently aggregate into highly stable and insoluble amyloid plaques. This $PrP^{Sc}$ plagess are resistant to digestion by proteinase K, whereas $PrP^C$ is sensitive to digestion by proteinase K (Prusiner 1998). $PrP^{Sc}$ is responsible for many diseases in humans, including Kuru, Gerstmann-Sträussler-Scheinker disease (GSS), fatal familial insomnia (FFI), Creutzfeldt-Jakob disease (CJD) and the BSE-related, variant Creutzfeldt-Jakob disease (vCJD) (Horwich & Weissman 1997; Prusiner 1997; Will et al. 1996). The infectious nature of these fatal diseases differ from other infectious diseases in that the pathogen is a proteinaceous particle rather than typical pathogens, such as viruses, bacteria and fungi. Therefore, a "protein-only" hypothesis has been proposed (Griffith 1967; Prusiner 1998). A protein designated as "protein X" has been proposed to be involved in structural conversion of $PrP^C$ into $PrP^{Sc}$ (Telling et al. 1995) in the protein-only model. After decades of study on prion proteins, protein X has not been identified. Thus, the mechanism of how $PrP^C$ is converted into $PrP^{Sc}$ remains ambiguous.

The structure of prion proteins has been studied in human (Calzolai & Zahn 2003; Donne et al. 1997; Zahn et al. 2000), hamster (James et al. 1997) and mouse sequences (Gossert et al.

2005; Riek et al. 1996). The structure of truncated mouse PrP (121-231) has been solved and reveals a α-helical protein containing 52% of α-helical and 3% of β-sheet structures (PDB code: 1AG2, (Riek et al. 1996)). Furthermore, NMR structure of hamster prion 90-231 reveals a flexible N-terminus and a structured C-terminal fragment (125-228) containing 43% of α-helical and 6% of β-sheet structures (PDB code: 1B10, (James et al. 1997)). The high flexibility of the N-terminus was confirmed in recombinant full-length hamster prion protein PrP 29-231 (Donne et al. 1997). The representative NMR structure of mouse prion is shown in Figure 1.

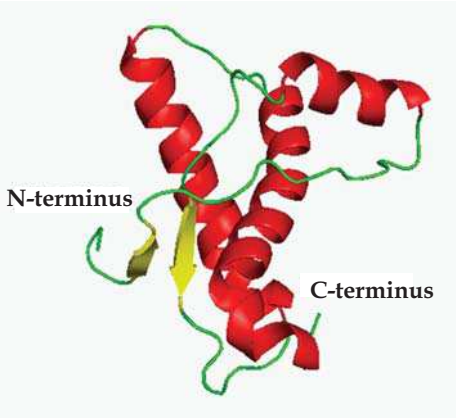


Fig. 1. The NMR structure of mouse prion protein (PDB code: 1AG2, (Riek et al. 1996)). The α-helical structures are represented by red ribbons, and the antiparallel β-sheet structure is colored in yellow. This figure was produced using the PyMol graphic package

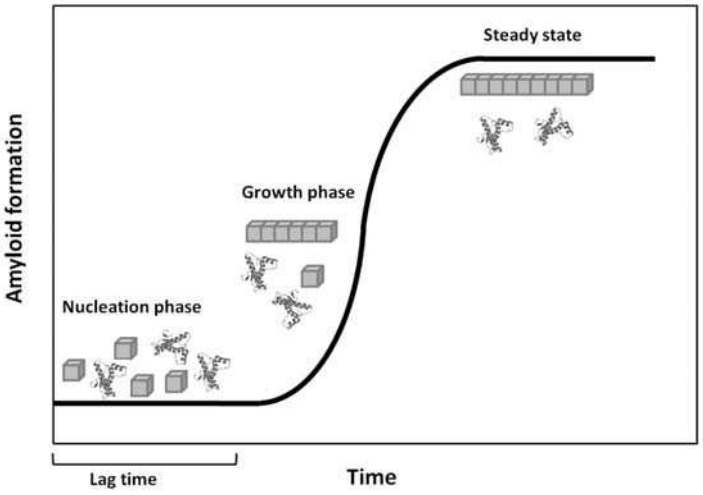


Fig. 2. Representative curve of nuclei-dependent polymerization model for amyloid formation

The formation of amyloid fibrils can be described by the polymerization model (Tsong & Baldwin 1972) illustrated in Figure 2. In this nucleation-dependent polymerization model, the conversion of proteins into nuclei that subsequently serve as seeds for amyloid fibrils is the rate-limiting step. Therefore, amyloid formation has a lag phase in which nucleation from protein monomers takes place. The spectroscopic signal for detecting amyloid fibrils is very weak during this nucleation phase, but the signal will enhance significantly during the fast polymerization catalyzed by the nuclei in the growth phase. Finally, the signal remains constant at a steady stateas that the ordered amyloid fibrils and protein monomers are at equilibrium.

In previous studies of recombinant PrP, a partially folded intermediate of PrP 90-231 has been suggested (Apetri et al. 2004; Kuwata et al. 2002; Nicholson et al. 2002). These partially unfolded states can potentially initiate amyloid formation (Abedini & Raleigh 2009; Chiti & Dobson 2009). Consequently, extensive works on the interaction of samll molecules and PrP have been conducted in order to find pharmacological chaperones that can stabilize the structure of $PrP^{C}$ (Nicoll et al. 2010). Chemical chaperones is an important target in the developments of therapies for prion disease. In the study of protein folding, osmolyte is a well-know factor that acts as a chemical chaperone to assist proteins to fold. Furthermore, cellular osmolarity can be changed by the ion-transportations. An increase in intracellular osmolarity caused by ion-transoprtation resulting astrocyte dysfunction in neurological disorders has been reviewed (Seifert et al. 2006). Therefore, it is essential to study osmolytes that affect folding of prion proteins. The chemical structure of the osmolyte trimethylamine N-oxide (TMAO) is illustrated in Figure 3 that TMAO is a zwitterionic compound at neutral pH, but is positively charged below pH 4.7 (Lin & Timasheff 1994). TMAO is a well known protective osmolyte that can increase structural stability of proteins against chemical or temperature-induced denaturation (Baskakov et al. 1998; Bolen & Baskakov 2001; Celinski & Scholtz 2002; Gursky 1999; Qu et al. 1998). TMAO has an extraordinary ability to force thermodynamically unstable proteins to fold (Baskakov & Bolen 1998). In contrast, TMAO destabilizes proteins at low pH (Singh et al. 2005).

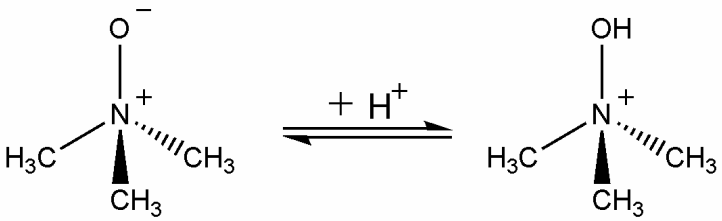


Fig. 3. Chemical structure of zwitterionic TMAO in equilibrium with its cationic form

A previous study by Tatzel and co-workers indicated that TMAO and the organic solvent dimethylsulfoxide (DMSO) prevent scrapie formation *in vitro* (Tatzelt et al. 1996). This study suggests a potential stratagy for preventing $PrP^{Sc}$ by stabilizing the conformation of $PrP^{C}$. In contrast, later studies indicated that TMAO destabilized the α-helical conformation of full-length human prion at neutral pH at high temperature (Nandi et al. 2006) and human prion proteins at low pH (Granata et al. 2006). The structure of α-helix-rich prion protein is destabilized and the prion protein is converted to β-sheet structured oligomeric species (Nandi et al. 2006).

In this study, we examined the effect of TMAO on conformational stability in full-length mouse prion proteins (MoPrPs) and their structural conversion to amyloid fibrils. A possible mechanism of TMAO on fibril formation is proposed based on the nucleation-dependent polymerization model.

## 2. Materials and methods

We characterized TMAO-induced structural change in MoPrP by circular dichroism spectroscopy and 8-anilino-1-naphthalenesulfonic acid (ANS)-binding fluorescence assay, and compared the effect of TMAO on the formation of amyloid fibrils by thioflavin T (ThT) binding assay and transmission electron microscopy (TEM).
Chemicals used in this work were purchased from Sigma Chemcial Co. (St. Louis, Missouri, USA), and used without further purification.

### 2.1 Protein expression and purification

Plasmid pET101 encoding mouse prion (23-231) was transformed into competent *E. coli* BL21 (DE3) and expressed in the form of inclusion bodies. The protein was purified on a Ni-sepharose column according to a previously described procedure (Bocharova et al. 2005). The purity of the isolated protein was confirmed by SDS-PAGE. The correct native conformation, containing mainly α-helical structures, was confirmed by circular dichroism spectroscopy.

### 2.2 Far-UV circular dichroism spectroscopy

Far-UV circular dichroism spectra of mouse prion was recorded with a J-815 (Jasco, Japan) spectropolarimeter equipped with a Peltier temperatue control system (model PTC 423). For measurements in the far-UV region, a quartz cell with a path length of 0.1 cm was used in nitrogen atmosphere. For protein samples, the concentration of MoPrP was kept constant at 10 μM in 10 mM 2-(*N*-morpholino)ethanesulfonic acid (MES, pH 6.0). Far-UV circular dichroism spectra between 200 and 250 nm were recorded. An accumulation of five scans with a scan speed of 50 nm per minute was performed at 20 °C. The thermal-induced denaturation of proteins was conducted by heating protein solutions at the rate of 1 °C/min, and measuring the molar ellipticity at 222 nm every 0.5 °C. The reading of molar ellipticity at 222 nm in accordance with temperature change was normalized for further analysis. The data were analyzed with Origin 6.0 from OriginLab (Northampton, Massachusetts, USA).

### 2.3 ANS fluorescence assay

ANS solution was added into 10 μM of TMAO-incubated MoPrP in 10 mM MES (pH 6.0) to a final concentration of 100 μM. For each sample, two fluorescence emission spectra were collected by a F-4500 fluorometer (Hitachi, Japan) with excitation either at 295 nm or 385 nm, respectively.

### 2.4 Fibril formation

Fibril conversion was conducted at 20 μM protein in the solution containing 2 M guanidine hydrochloride (GdnHCl) and 50 mM MES (pH 6) at 37 °C as described in a previous study on mouse prion fibrils (Bocharova et al. 2005). At the end of the experiments, the fibril samples were dialyzed against 20 mM sodium acetate (pH 5.5) for further experiments.

### 2.5 ThT fluorescence assay of fibril conversion

Aliquots withdrawn during the time course of incubation at 37 °C were diluted into 5 mM sodium acetate buffer (pH 5.5) to a final sample concentration of 0.5 μM. ThT solution was added to a final concentration of 10 μM. For each sample, two emission spectra were collected by a F-4500 fluorometer (Hitachi, Japan) equipped with a 150 W Xenon lamp. The fluorescence spectra were recorded from 470 to 550 nm with excitation wavelength of 450 nm. The maximum fluorescence emission at 482 nm was determined. The reported fluorescence readings were average values for two measurements.

### 2.6 TEM

The aliquotes of mouse prion fibril samples were stained with 2% tungsten phosphoric acid onto carbon-coated 200-mesh copper grids. The samples were adsorbed onto copper grids for 30 sec and subsequently washed with PBS and $mQH_2O$. The samples were air-dried before imaging. The TEM images were collected by a H-7100 TEM (Hitachi, Japan). The analysis of fibril length and width was carried out on WICF ImageJ software (National Institutes of Health).

## 3. Results and discussion

We characterized the effect of the osmolyte TMAO on the structure of MoPrP by far-UV circular dichroism spectroscopy and ANS-binding fluorescence assay. Furthermore, we tested the effect of TMAO on amyloid fibril formation. The prion fibrils grown at different concentrations of TMAO were analyzed by TEM.

### 3.1 Secondary structure and protein stability

We collected far-UV circular dichroism spectra for MoPrP at pH 6.0 at 20 °C. As shown in Figure 4, MoPrP has the typical feature of α-helical conformation as indicated by the circular dichroic signals at 208 nm and 222 nm. In prior investigations of TMAO and its effects on MoPrP structure, circular dichroism spectra of MoPrP in 2 M TMAO were recorded every hour. These spectra collected within 6 hours are very similar (data not shown). Since the extension of incubation does not affect the structural features of MoPrP, the following spectroscopic experiments were conducted without prolonged incubation.

#### 3.1.1 TMAO causes unfolding and destabilizes MoPrP

We investigated the addition of TMAO in the range of 0.5 ~ 2 M and its effect on MoPrP using circular dichroism spectroscopy. The results are presented in Figure 4A. Osmolyte TMAO exhibits substantial interference below 205 nm. Therefore, the interfering circular dichroic signal was removed from the plot. In the absence of TMAO, MoPrP has clear circular dichroic feature of α-helical conformation at 208 and 222 nm. After addition of 0.5 M and 1.0 M TMAO, the circular dichroic signal indicative of α-helix structure at 208 nm decreased slightly, while the signal at 222 nm remained generally unchanged. Significantly, addition of 1.5 M and 2.0 M weakens the entire α-helical conformation. The unfolding of α-helical structure has been reported with similar work performed at low pH (Granata et al. 2006). Consistently, the significant unfolding of prion proteins is carried out at > 1.0 M TMAO as illustrated in Figure 4B. Differently, the dichroic signal at 208 nm is affected by TMAO more severely than that at 222 nm. The dichroic signal at 208 nm dominants the dichroic curve of α-helix in the absence of TMAO, but this signal is largely weakened by the

addition of TMAO. The dichroic curve of TMAO-affected partially folded α-helical structure observed in this work is not identical to the curves observed in the similar work performed at high temperature (Nandi et al. 2006). These results indicated that TMAO affect the structure of prion proteins differently under different conditions. At neutral pH, TMAO is zwitterionic, but it becomes cationic at low pH. Full-length prion protein includes polybasic N-terminal region 23-30 which is essential for effective folding into the native cellular conformation (Ostapchenko et al. 2008). Therefore, the differentiation of TMAO-induced conformational change at different pH values can be partially, if not all, ascribed to the interaction between TMAO and the polybasic N-terminal region.

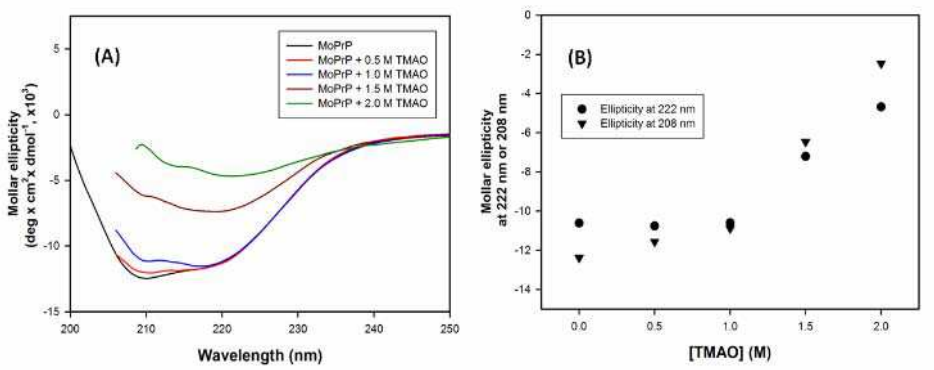


Fig. 4. (A) Far-UV circular dichroism spectra of 10 μM MoPrP measured after the addition of TMAO. (B) Comparison of mollar ellipticity at 222 nm and 208 nm in various concentration of TMAO

TMAO is known to increase the melting temperature of various proteins (Arakawa & Timasheff 1985). Therefore, in addition to the conformation change, the structural stability of MoPrP in the presence of TMAO was examined with thermal-induced denaturation monitored by the molar ellipticity at 222 nm. The molar ellipticity was normalized to represent the fraction of unfolded proteins as presented in Figure 5.

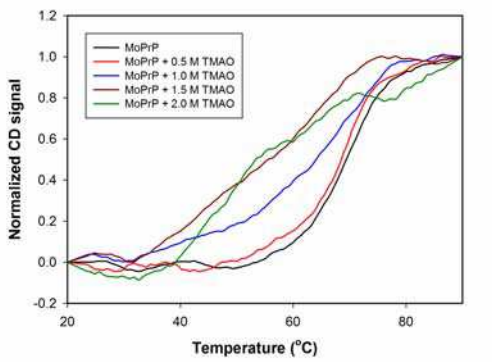


Fig. 5. Thermal-induced denaturation of MoPrP monitored the circular dichroic signal at 222 nm

The curves of heat-induced denaturation can be described by a cooperative two-state model of denaturation in which proteins are transited between natively folded states and denatured unfolded states. By monitoring the circular dichroic signal at 222 nm, the natively folded MoPrP has the minimum intensity, whereas fully unfolded proteins has the maximum readings. These denaturation curves can be analyzed based on the Gibbs-Helmholtz equation:

$$\Delta G_U^\circ(T) = \Delta H°(T_m)(1 - \frac{T}{T_m}) - \Delta G_p^\circ[(T_m - T) + T\ln(\frac{T}{T_m})] \quad (1)$$

Based on the above equation, the melting temperature ($T_m$) of MoPrP can be determine. In the absence of TMAO, the $T_m$ of MoPrP is 68.63 °C. Addition of 0.5 M TMAO does not affect the thermal-denaturation curve significantly, as the $T_m$ value was calculated to be 68.19 °C. In the presence of 1.0 ~ 1.5 M TMAO, the thermal-denaturation curve shifted toward low temperature significantly, as MoPrP starts to denature at ~32 °C. In contrast to the denaturation curve collected in the absence of TMAO, the thermal-denaturation curves of MoPrP treated with ≥ 1.0 M TMAO are not typical of cooperative two-state unfolding. These curves implies that TMAO changes the unfolding pathway, and that more intermediates are present at high concentration of TMAO.

### 3.2 TMAO-induced conformational change within the native state

The hydrophobic dye ANS has been widely used to detect the conformational changes in proteins, as ANS preferentially binds to hydrophobic protein surfaces. The binding of ANS to hydrophobic area causes significant increase in the fluorescence emission of ANS. Therefore, we detected ANS fluorescence emission upon excitation at at 385 nm to detect the change of hydrophobicity of MoPrP as presented in Figure 6. Clearly, ANS-bound MoPrP emits fluorescence at 470 nm and 495 nm upon excitation at 385 nm which indicates the presence of two distinct ANS-binding pockets. Addition of 0.5 M TMAO weakens the fluorescence emission of ANS slightly, but addition of 1.0 ~ 2.0 M TMAO substantially increased ANS fluorescence. The increase of ANS emission at 470 nm is more pronounced than the fluorescence at 495 nm. It indicates that the hydrophobicity represents by 470 nm is more sensitive to TMAO than the other one at 495 nm. Overall, this result indicates that TMAO increases hydrophobic surface at two distinct sites in MoPrP.

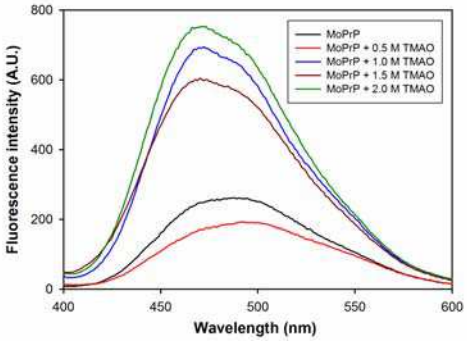


Fig. 6. Fluorescence of ANS in the absence and in the presence of TMAO upon excitation at 385 nm

In addition to the change of hydrophobicity in MoPrP, we detected ANS fluorescence emission upon excitation at 295 nm to study the TMAO-induced conformational change. Excitation at 295 nm excites tryptophan (Trp) and ANS at the same time, but this excitation causes the energy transfer from Trp (donor) in the N-terminus to ANS (acceptor). As the energy transfer efficiency (E) is determined by the distance of donor-acceptor (r) in the relation of $E \alpha r^{-6}$, the fluorescence spectra with excitation at 295 nm provide the distance information between Trp and ANS-bound residues. As illustrated in Figure 7, in the absence of TMAO, MoPrP has fluorescence emission at 350 nm and 485 nm arising from Trp and ANS-binding, respectively. Upon the addition of TMAO, the energy in Trp transfers to MoPrP-bound ANS efficiently that the signal of Trp at 350 nm is completely abolished, and the fluorescence of ANS is significantly enhanced. The fluorescence spectra of ANS in the presence of TMAO illustrate a strong peak at 408 nm, a medium, broad peak at ~460 nm and a weak, broad peak at ~490 nm overlapped with the broad peak at 460 nm. The fluorescence at 490 nm is a typical emission of ANS-binding as observed in Figure 6. This weak signal at 490 nm could be ascribed to MoPrP-bound ANS molecules that do not accept energy from Trp efficiently. As the addition of TMAO causes the peaks at 408 nm and at 460 nm to increase at different degrees, it is predicted that there are two distinct hydrophobic pockets near the N-terminal region but away from Trp with different distances.

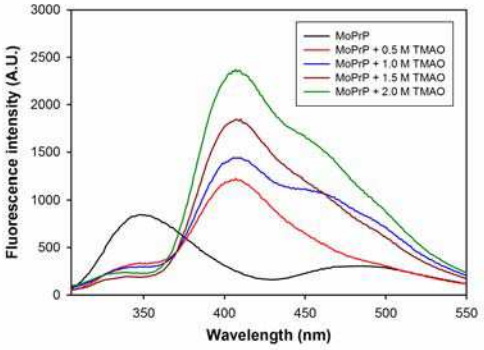


Fig. 7. Fluorescence of ANS in the absence and in the presence of TMAO upon excitation at 295 nm

### 3.2 Fibril conversion in TMAO

Partially unfolded MoPrP can potentially initiate formation of amyloid fibrils (Abedini & Raleigh 2009; Chiti & Dobson 2009). In 2 M GdnHCl, MoPrP is about half folded and is readily converted into amyloid fibrils (Breydo et al. 2005). Formation of amyloid fibrils can be monitored by ThT-binding fluorescence because the fluorescence of ThT is greatly enhanced when ThT binds to β-sheet rich structures, which are the main structures found in the amyloid fibrils (LeVine 1999). Therefore, the intensity of ThT-binding fluorescence represents the amount of amyloid fibrils converted from protein monomers in the absence of TMAO. As illustrated in Figure 8, the kinetics of fibril conversion shows sigmoidal curves. The MoPrP starts to form amyloid fibrils after 6 hours of incubation as monitored by ThT-binding fluorescence. The prion fibrils grow rapidly such that the maximum ThT fluorescence reached ~400 after 8 hours of amyloid fibril conversion. In the presence of 0.5

or 1.0 M of TMAO, the amyloid fibrils grow very well such that the maximum values of ThT fluorescence are higher in comparison to those in the absence of TMAO. When the concentration of TMAO is increased to 1.5 M and above, MoPrP rarely converts to amyloid fibrils as indicated by low ThT-binding fluorescence.

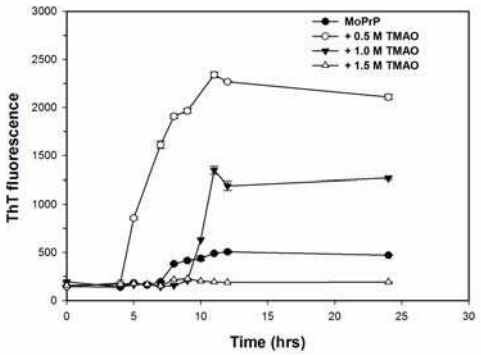


Fig. 8. Kinetic traces for amyloid fibril formation from MoPrP monitored by ThT-binding fluorescence in the presence of 2 M GdnHCl and various concentrations of TMAO at pH 6.0 at 37 °C. The fluorescence readings were average values of two measurements

The quantity of prion fibrils judged by the maximum ThT fluorescence in the presence of TMAO is presented in Figure 9A. Clearly, addition of 0.5 and 1.0 M TMAO promotes amyloid formation as the reading of ThT-fluorescence is greatly enhanced in comparison to that in the absence of TMAO. In contrast, when the concentration of TMAO was increased further, the fibril conversion was inhibited. It is interesting to observe enhancement of fibril conversion by TMAO at ≤ 1.0 M. This result is consistent with previous work performed on α-synuclein that 1.0 M TMAO yields large amount of fibril whereas 2.0 and 3.0 M of TMAO inhibits the fibril formation (Uversky et al. 2001).

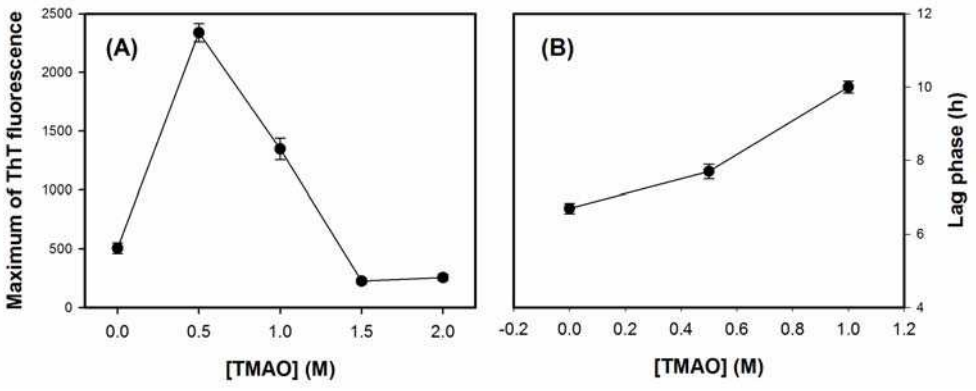


Fig. 9. (A)The quantity of amyloid fibrils converted from MoPrP monitored by the maximum of ThT-binding fluorescence measured two times, and (B) the calculated lag phase of fibril conversion in the absence and in the presence of TMAO

The formation of amyloid fibrils in the presence of 0 ~ 1.5 M TMAO follows the nucleation-dependent polymerization model as illustrated in Figure 2. According to this nucleation-dependent polymerization model, the lag phase of amyloid formation from MoPrP can be determined by fitting the time-dependent changes in the ThT fluorescence (F) over time (t) of the reaction as shown in the following equation (Bocharova et al. 2005):

$$F = F_0 + \frac{\Delta F}{1 + \exp[k(t_m - t)]} \tag{2}$$

Where $F_0$ is the minimum level of ThT fluorescence during the lag phase, $\Delta F$ is the difference of ThT fluorescence between the maximum level (steady state) and the minimum level (lag phase), k is the rate constant of fibril growth ($h^{-1}$), and $t_m$ is the observed time at the midpoint of transition. The lag time ($t_l$) of fibril formation can be calculated as:

$$t_l = t_m - \frac{2}{k} \tag{3}$$

According to these two equations, the lag time for fibril formation in the presence of 0, 0.5 and 1.0 M TMAO was determined as presented in Figure 9B. Previous work on fibril conversion from α-synuclein in the presence of TMAO reported acceleration of amyloid formation in a wide range of TMAO concentration (1.0 ~ 3.0 M) due to osmolyte-induced stabilization of the partially folded intermediate (Uversky et al. 2001). Similarly, TMAO stabilizes some partially folded intermediates. However, these partially folded intermediates slightly disfavour the nucleation reaction resulting in slight extension of the nucleation phase and also the following growth phase.

### 3.3 Morphology of prion fibrils grown with TMAO

Variation of conditions for fibril formation from the identical protein can yield different morphology. For example, Makarava and Baskakov have observed curved and straight fibrils from the same mouse prion protein and identical solvent conditions but different in the shaking speed (Makarava & Baskakov 2008). Therefore, we investigated the morphology of mouse prion fibrils by electron microscopy. In our experiment, for mature mouse prion fibrils grown in 2 M GdnHCl, the length is mostly longer than 500 nm, and the width is about 20 nm as illustrated in Figure 10.

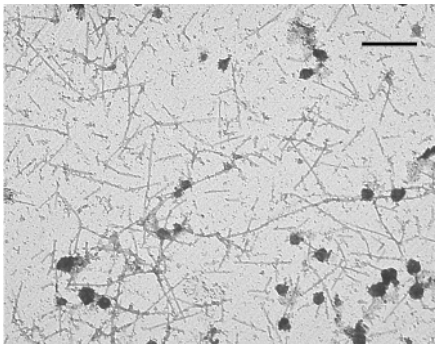

Fig. 10. TEM image of mature prion fibrils grown in 2 M GdnHCl at pH 6.0 at 37 °C. The scale bar represents 500 nm

The growth phase of fibril conversion in the absence of TMAO is very short, whereas this elongation process takes longer in the addition of TMAO. To compare the morphology of prion fibrils during elongation in the absence and in the presence of TMAO, we collected TEM images of fibril samples in the middle point of growth phase. As illustrated in Figure 11, the prion fibrils grown in the absence of TMAO are long and straight, whereas fibrils converted in the presence of TMAO look like short rods.

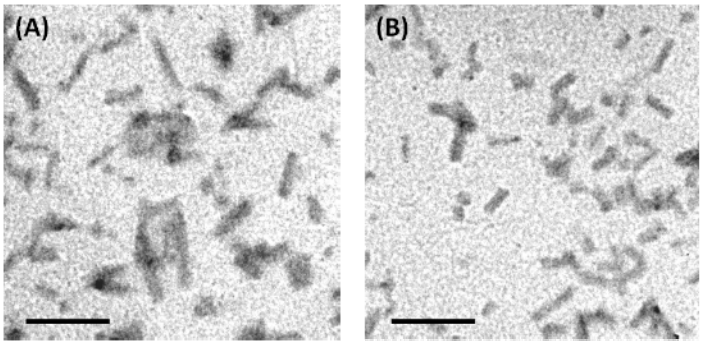


Fig. 11. TEM images of mouse prion fibrils at the middle point of growth phase (A) in the absence of TMAO and (B) in the presence of 1.0 M TMAO. The scale bar represents 200 nm

Oligomers, protofibrils and mature fibrils involved in the formation of amyloid fibrils are typically distinguished by the length and width of the fibrils. Therefore, we statistically compared the length and the width of prion fibrils converted in the absence and in the presence of 0.5 M and 1.0 M TMAO. As illustrated in Figure 12A, in the absence of TMAO, the fibril length is populated in two groups including one normal distribution between 60 ~ 180 nm and an elongation at > 180 nm. Prion fibrils with the addition of 0.5 M TMAO are normally distributed between 20 ~ 160 nm and the most populated length is 80 ~ 120 nm. Increasing TMAO to 1.0 M shortens the prion fibrils, so that the fibril length ranges from 20 to 140 nm with the most populated length being 40 ~ 60 nm. The average length of prion fibrils is 144 nm in the absence of TMAO. Addition of TMAO shortens the average length of prion fibrils to 92 and 61 nm in the presence of 0.5 M and 1.0 M, respectively. In contrast to the fibril length, the width of prion fibrils is similar as illustrated in Figure 12B, and the average of the width is 19 nm regardless the presence of TMAO.

The structural effect of osmolyte TMAO on prion proteins and fibril conversion has been investigated extensively in this work. At pH 6.0, 20 °C, the α-helical conformation of MoPrP is unfolded by TMAO. When the concentration of TMAO is low at ≤ 1.0 M, the degree of unfolding is small and the fibril conversion takes place on the mostly folded α-helical structures. In contrast to low concentration of TMAO, high concentration of TMAO at >1.0 M largely unfolds the α-helix and this unfolding inhibits amyloid formation completely. In other words, low concentration of TMAO decellarates the prion nucleation represented by lag phase in nucleation-dependent polymerization model, whereas TMAO enhances the growth of prion fibrils. This contrast effect indicates that the structural requirement of prion proteins in nucleation and in fibril elongation is different. The importance of partial unfolding of prion in amyloid formation has been suggested (Apetri et al. 2004; Kuwata et al. 2002; Nicholson et al. 2002). The structure of partially folded prion protein that initiates amyloid formation remains unclear. Our recent computational simulation proposed that the

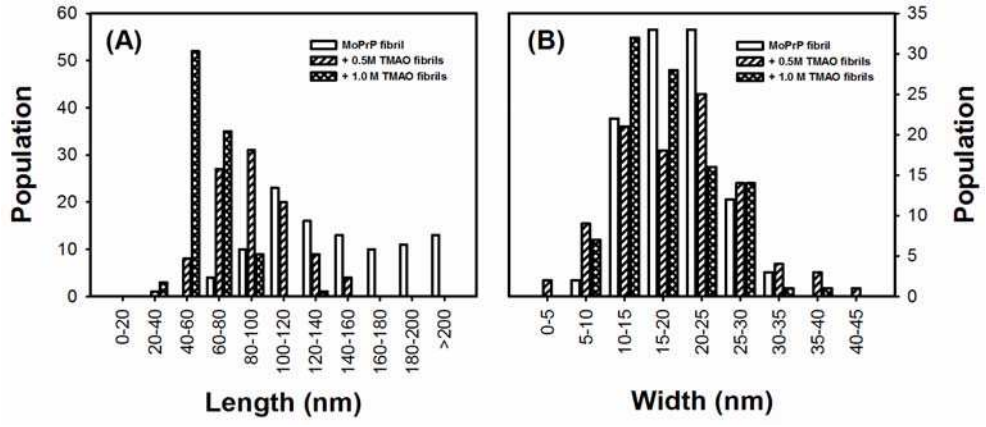


Fig. 12. Histrogram of length and width of prion fibrils measured on 100 fibrils in the absence and in the presence of 0.5 M and 1.0 M TMAO

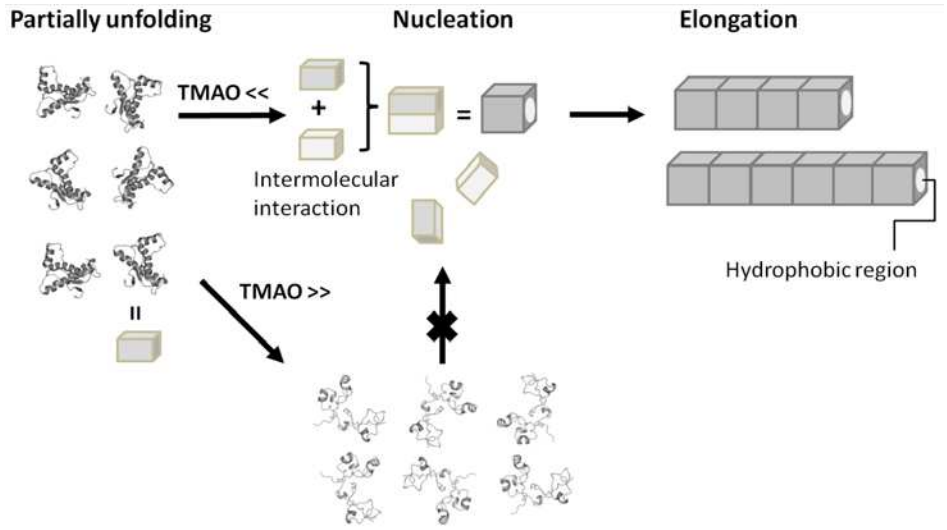


Fig. 13. A scheme illustrating the proposed effect of TMAO based on nucleation-dependent polymerization model

denatured state of prion protein is partially folded with α-helical conformation (Lee & Chang 2010). In prion nucleation, high α-helical conformation is preferred and intermolecular β-sheet interactions occur between prion monomers (Lee et al. 2010). This interaction of intermolecular β-sheets is most likely the initiation of nucleation. This intermolecular interaction might be correlated with a double-layered filament within one fibril as observed by atomic force microscopy (Anderson et al. 2006). When the α-helical structure is mostly lost and the intermolecular interaction is largely weakened, the amyloid formation can not take place due to failure of nucleation as illustrated in Figure 13. After

nuclei are formed as fibril seeds, the elongation requires stable interactions between nuclei and proteins. As amyloid fibrils have been proposed to have hydrophobic interior (Buchete & Hummer 2007; Carroll et al. 2006), the area of the hydrophobic surface is important in fibril elongation. The hydrophobicity at the ANS-binding pockets that accept energy from Trp is induced significantly by TMAO, and the high hydrophobicity promotes hydrophobic interactions of nuclei and proteins to form the hydrophobic interior. Notably, in the presence of low concentration of TMAO, the amount of fibrils is significantly increased, but the fibril length is shortened in the middle of growth phase. This phenomenon could be due to adjustment of interaction between nuclei under high hydrophobicity as judged by long growth phase in the presence of TMAO. Taking togther these findings, a certain amount of α-helical conformation seems to be required in the structural conversion of prion proteins in nucleation, and hydrophobic interaction is essential in fibril elongation.

## 4. Conclusion

In this study, we have investigated the structural effect of osmolytes TMAO on MoPrP proteins and the features of mouse prion fibrils. Low concentration of TMAO alters α-helical structures resulting deceleration of nucleation serving as fibril seeds, but TMAO enhances hydrophobicity promoting fibril growth. High concentration of TMAO inhibits amyloid formation completely by inducing loss of α-helical conformation. This study provides more information in the details of molecular structure and interaction in amyloid formation. These findings are essential in further search for therapeutic therapies for prion disease.

## 5. Acknowledgment

We are grateful to National Science Council for financial support (Project 100-2321-B-194-001). We also thank Dr. Raymond Chung for editing the manuscript. Usage of PyMol graphics packages and WICF ImageJ software is gratefully acknowledged.

## 6. References

Abedini, A. and Raleigh, D. P. (2009). A role for helical intermediates in amyloid formation by natively unfolded polypeptides? *Phys Biol*, 6, 1, 15005.

Anderson, M., Bocharova, O. V., Makarava, N., et al. (2006). Polymorphism and ultrastructural organization of prion protein amyloid fibrils: an insight from high resolution atomic force microscopy. *J Mol Biol*, 358, 2, 580-596.

Apetri, A. C., Surewicz, K. and Surewicz, W. K. (2004). The effect of disease-associated mutations on the folding pathway of human prion protein. *J Biol Chem*, 279, 17, 18008-18014.

Arakawa, T. and Timasheff, S. N. (1985). The stabilization of proteins by osmolytes. *Biophys J*, 47, 3, 411-414.

Baskakov, I. and Bolen, D. W. (1998). Forcing thermodynamically unfolded proteins to fold. *J Biol Chem*, 273, 9, 4831-4834.

Baskakov, I., Wang, A. and Bolen, D. W. (1998). Trimethylamine-N-oxide counteracts urea effects on rabbit muscle lactate dehydrogenase function: a test of the counteraction hypothesis. *Biophys J*, 74, 5, 2666-2673.

Bocharova, O. V., Breydo, L., Salnikov, V. V., et al. (2005). Copper(II) inhibits in vitro conversion of prion protein into amyloid fibrils. *Biochemistry*, 44, 18, 6776-6787.

Bocharova, O. V., Breydo, L., Salnikov, V. V., et al. (2005). Synthetic prions generated in vitro are similar to a newly identified subpopulation of PrPSc from sporadic Creutzfeldt-Jakob disease. *Protein Sci*, 14, 5, 1222-1232.

Bolen, D. W. and Baskakov, I. V. (2001). The osmophobic effect: natural selection of a thermodynamic force in protein folding. *J Mol Biol*, 310, 5, 955-963.

Breydo, L., Bocharova, O. V., Makarava, N., et al. (2005). Methionine oxidation interferes with conversion of the prion protein into the fibrillar proteinase K-resistant conformation. *Biochemistry*, 44, 47, 15534-15543.

Brown, D. R., Schmidt, B. and Kretzschmar, H. A. (1998). Effects of copper on survival of prion protein knockout neurons and glia. *J Neurochem*, 70, 4, 1686-1693.

Buchete, N. V. and Hummer, G. (2007). Structure and dynamics of parallel beta-sheets, hydrophobic core, and loops in Alzheimer's A beta fibrils. *Biophys J*, 92, 9, 3032-3039.

Calzolai, L. and Zahn, R. (2003). Influence of pH on NMR structure and stability of the human prion protein globular domain. *J Biol Chem*, 278, 37, 35592-35596.

Carroll, A., Yang, W., Ye, Y., et al. (2006). Amyloid fibril formation by a domain of rat cell adhesion molecule. *Cell Biochem Biophys*, 44, 2, 241-249.

Celinski, S. A. and Scholtz, J. M. (2002). Osmolyte effects on helix formation in peptides and the stability of coiled-coils. *Protein Sci*, 11, 8, 2048-2051.

Chiti, F. and Dobson, C. M. (2009). Amyloid formation by globular proteins under native conditions. *Nat Chem Biol*, 5, 1, 15-22.

Donne, D. G., Viles, J. H., Groth, D., et al. (1997). Structure of the recombinant full-length hamster prion protein PrP(29-231): the N terminus is highly flexible. *Proc Natl Acad Sci U S A*, 94, 25, 13452-13457.

Gossert, A. D., Bonjour, S., Lysek, D. A., et al. (2005). Prion protein NMR structures of elk and of mouse/elk hybrids. *Proc Natl Acad Sci U S A*, 102, 3, 646-650.

Granata, V., Palladino, P., Tizzano, B., et al. (2006). The effect of the osmolyte trimethylamine N-oxide on the stability of the prion protein at low pH. *Biopolymers*, 82, 3, 234-240.

Griffith, J. S. (1967). Self-replication and scrapie. *Nature*, 215, 5105, 1043-1044.

Gursky, O. (1999). Probing the conformation of a human apolipoprotein C-1 by amino acid substitutions and trimethylamine-N-oxide. *Protein Sci*, 8, 10, 2055-2064.

Horwich, A. L. and Weissman, J. S. (1997). Deadly conformations--protein misfolding in prion disease. *Cell*, 89, 4, 499-510.

James, T. L., Liu, H., Ulyanov, N. B., et al. (1997). Solution structure of a 142-residue recombinant prion protein corresponding to the infectious fragment of the scrapie isoform. *Proc Natl Acad Sci U S A*, 94, 19, 10086-10091.

Kuwata, K., Li, H., Yamada, H., et al. (2002). Locally disordered conformer of the hamster prion protein: a crucial intermediate to PrPSc? *Biochemistry*, 41, 41, 12277-12283.

Lee, C. I. and Chang, N. Y. (2010). Characterizing the denatured state of human prion 121-230. *Biophys Chem*, 151, 1-2, 86-90.

Lee, S., Antony, L., Hartmann, R., et al. (2010). Conformational diversity in prion protein variants influences intermolecular beta-sheet formation. *EMBO J*, 29, 1, 251-262.

LeVine, H., 3rd (1999). Quantification of beta-sheet amyloid fibril structures with thioflavin T. *Methods Enzymol*, 309, 274-284.

Lin, T. Y. and Timasheff, S. N. (1994). Why do some organisms use a urea-methylamine mixture as osmolyte? Thermodynamic compensation of urea and trimethylamine N-oxide interactions with protein. *Biochemistry*, 33, 42, 12695-12701.

Makarava, N. and Baskakov, I. V. (2008). The same primary structure of the prion protein yields two distinct self-propagating states. *J Biol Chem*, 283, 23, 15988-15996.

Mouillet-Richard, S., Ermonval, M., Chebassier, C., et al. (2000). Signal transduction through prion protein. *Science*, 289, 5486, 1925-1928.

Nandi, P. K., Bera, A. and Sizaret, P. Y. (2006). Osmolyte trimethylamine N-oxide converts recombinant alpha-helical prion protein to its soluble beta-structured form at high temperature. *J Mol Biol*, 362, 4, 810-820.

Nicholson, E. M., Peterson, R. W. and Scholtz, J. M. (2002). A partially buried site in homologous HPr proteins is not optimized for stability. *J Mol Biol*, 321, 2, 355-362.

Nicoll, A. J., Trevitt, C. R., Tattum, M. H., et al. (2010). Pharmacological chaperone for the structured domain of human prion protein. *Proc Natl Acad Sci U S A*, 107, 41, 17610-17615.

Ostapchenko, V. G., Makarava, N., Savtchenko, R., et al. (2008). The polybasic N-terminal region of the prion protein controls the physical properties of both the cellular and fibrillar forms of PrP. *J Mol Biol*, 383, 5, 1210-1224.

Prusiner, S. B. (1982). Novel proteinaceous infectious particles cause scrapie. *Science*, 216, 4542, 136-144.

Prusiner, S. B. (1997). Prion diseases and the BSE crisis. *Science*, 278, 5336, 245-251.

Prusiner, S. B. (1998). Prions. *Proc Natl Acad Sci U S A*, 95, 23, 13363-13383.

Qu, Y., Bolen, C. L. and Bolen, D. W. (1998). Osmolyte-driven contraction of a random coil protein. *Proc Natl Acad Sci U S A*, 95, 16, 9268-9273.

Riek, R., Hornemann, S., Wider, G., et al. (1996). NMR structure of the mouse prion protein domain PrP(121-321). *Nature*, 382, 6587, 180-182.

Seifert, G., Schilling, K. and Steinhauser, C. (2006). Astrocyte dysfunction in neurological disorders: a molecular perspective. *Nat Rev Neurosci*, 7, 3, 194-206.

Singh, R., Haque, I. and Ahmad, F. (2005). Counteracting osmolyte trimethylamine N-oxide destabilizes proteins at pH below its pKa. Measurements of thermodynamic parameters of proteins in the presence and absence of trimethylamine N-oxide. *J Biol Chem*, 280, 12, 11035-11042.

Tatzelt, J., Prusiner, S. B. and Welch, W. J. (1996). Chemical chaperones interfere with the formation of scrapie prion protein. *EMBO J*, 15, 23, 6363-6373.

Telling, G. C., Scott, M., Mastrianni, J., et al. (1995). Prion propagation in mice expressing human and chimeric PrP transgenes implicates the interaction of cellular PrP with another protein. *Cell*, 83, 1, 79-90.

Tsong, T. Y. and Baldwin, R. L. (1972). A sequential model of nucleation-dependent protein folding: kinetic studies of ribonuclease A. *J Mol Biol*, 63, 3, 453-469.

Uversky, V. N., Li, J. and Fink, A. L. (2001). Trimethylamine-N-oxide-induced folding of alpha-synuclein. *FEBS Lett*, 509, 1, 31-35.

Whittal, R. M., Ball, H. L., Cohen, F. E., et al. (2000). Copper binding to octarepeat peptides of the prion protein monitored by mass spectrometry. *Protein Sci*, 9, 2, 332-343.

Will, R. G., Ironside, J. W., Zeidler, M., et al. (1996). A new variant of Creutzfeldt-Jakob disease in the UK. *Lancet*, 347, 9006, 921-925.

Zahn, R., Liu, A., Luhrs, T., et al. (2000). NMR solution structure of the human prion protein. *Proc Natl Acad Sci U S A*, 97, 1, 145-150.

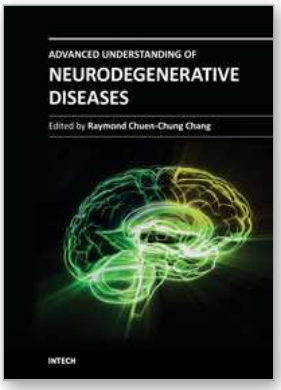


**Advanced Understanding of Neurodegenerative Diseases**

Edited by Dr Raymond Chuen-Chung Chang

ISBN 978-953-307-529-7
Hard cover, 442 pages
**Publisher** InTech
**Published online** 16, December, 2011
**Published in print edition** December, 2011

Advanced Understanding of Neurodegenerative Diseases focuses on different types of diseases, including Alzheimer's disease, frontotemporal dementia, different tauopathies, Parkinson's disease, prion disease, motor neuron diseases such as multiple sclerosis and spinal muscular atrophy. This book provides a clear explanation of different neurodegenerative diseases with new concepts of understand the etiology, pathological mechanisms, drug screening methodology and new therapeutic interventions. Other chapters discuss how hormones and health food supplements affect disease progression of neurodegenerative diseases. From a more technical point of view, some chapters deal with the aggregation of prion proteins in prion diseases. An additional chapter to discuss application of stem cells. This book is suitable for different readers: college students can use it as a textbook; researchers in academic institutions and pharmaceutical companies can take it as updated research information; health care professionals can take it as a reference book, even patients' families, relatives and friends can take it as a good basis to understand neurodegenerative diseases.



**InTech Europe**
University Campus STeP Ri
Slavka Krautzeka 83/A
51000 Rijeka, Croatia
Phone: +385 (51) 770 447
Fax: +385 (51) 686 166
www.intechopen.com

**InTech China**
Unit 405, Office Block, Hotel Equatorial Shanghai
No.65, Yan An Road (West), Shanghai, 200040, China
中国上海市延安西路65号上海国际贵都大饭店办公楼405单元
Phone: +86-21-62489820
Fax: +86-21-62489821